Solution Structure of Bovine Neutrophil β-Defensin-12: The Peptide Fold of the β-Defensins Is Identical to That of the Classical Defensins[†,||]

Grant R. Zimmermann,[‡] Pascale Legault,[‡] Michael E. Selsted,[§] and Arthur Pardi*[,‡]

Department of Chemistry and Biochemistry, University of Colorado at Boulder, Boulder, Colorado 80309-0215, and Departments of Pathology, Microbiology and Molecular Genetics, University of California College of Medicine, Irvine, California 92717

Received May 8, 1995; Revised Manuscript Received August 23, 1995[⊗]

ABSTRACT: The solution structure is reported for bovine neutrophil β-defensin-12 (BNBD-12), a member of the β-defensin family of antimicrobial peptides. Structural constraints in the form of proton−proton distances, dihedral angles, and hydrogen bond constraints were derived from two-dimensional, homonuclear magnetic resonance spectroscopy experiments. The three-dimensional structure of BNBD-12 was calculated using distance geometry and restrained molecular dynamics. An ensemble of structures with low NOE constraint violation energies revealed a precisely defined triple-stranded, antiparallel β-sheet as the structural core of the peptide. The N-terminal β-strand and three locally well-defined tight turns form a hydrophobic face. Conserved isoleucine and glycine residues form a β-bulge structure which initiates a β-hairpin secondary structure motif composed of the second and C-terminal β-strands. The β-hairpin contains numerous charged residues and forms the cationic face of BNBD-12. The N-terminal residues were found to be disordered, due to an absence of tertiary NOEs. The triple-stranded β-sheet, the β-bulge preceding the hairpin, and the cationic/hydrophobic amphiphilic character are definitive features of all defensin structures determined to date. Further, we predict that the tracheal antimicrobial peptide (TAP) and the recently described gallinacins will have tertiary structures similar to that of BNBD-12.

The classical defensins are a well-characterized class of antimicrobial peptides isolated from the azurophilic granules of polymorphonuclear leukocytes and macrophages. These peptides are part of the oxygen-independent pathway used by leukocytes and macrophages to kill ingested organisms. The peptides are 29−35 amino acids in length and are variably cationic. Defensins share a unique disulfide-bonding motif of six conserved cysteines (Lehrer et al., 1993; Selsted & Harwig, 1989). The defensins were identified by virtue of their antimicrobial activity in the leukocytes or macrophages of humans, rabbits, rats, and guinea pigs, and the Paneth cells of mouse small intestine (Eisenhauer et al., 1989; Ganz et al., 1985; Ouellette et al., 1992; Selsted et al., 1985; Selsted & Harwig, 1987). Some defensins have also been shown to bind specifically to adrenocorticotrophin receptors and to be chemotactic for human monocytes (Territo et al., 1989; Tominaga et al., 1990). A number of defensins from human and rabbit have been studied structurally in solution or in a single crystal (Bach et al., 1987; Hill et al., 1991; Pardi et al., 1988, 1992; Zhang et al., 1992).

BNBD-12[1] is a member of a family of 13 structurally related peptides isolated from bovine neutrophils that possess antimicrobial activity against *Escherichia coli* and *Staphylococcus aureus* (Selsted et al., 1993). This family, termed the β-defensins, has many properties in common with the well-characterized classical defensins such as broad spectrum antimicrobial activity, three disulfide linkages, and a large number of arginine residues (Selsted et al., 1993). TAP isolated from bovine trachea shares a high degree of sequence similarity with the β-defensins (Diamond et al., 1991). A family of antimicrobial peptides, termed gallinacins, remarkably similar to the β-defensins has recently been isolated from chicken leukocytes (Harwig et al., 1994). The gallinacins, β-defensins, and TAP have nearly identical spacing of their conserved six cysteine residues, are both arginine and lysine rich, and also share three additional conserved residues.

The small size of BNBD-12 with 38 amino acids and the high stability imparted by the three disulfide bonds make it an ideal molecule for investigation by homonuclear magnetic resonance techniques. A unique disulfide-bonding motif relative to the classical defensins was determined biochemically for BNBD-12 (Tang & Selsted, 1993). The differences in size (38−42 amino acids for the β-defensins), primary

[†] This work was supported in part by funds from NIH Grant AI 27026, a NIH Research Career Development Award AI 01051 to A.P., and NIH Grants AI 22931 and AI 31696 to M.E.S. P.L. was supported by a NSERC 1967 Science and Engineering scholarship and a FCAR (Fonds pour la Formation de Chercheurs et l' Aide a la Recherche) scholarship. The VXR-S 500 MHz NMR spectrometer was purchased with partial support from NIH Grant RR 03283.

* Author to whom correspondence should be addressed.

[‡] University of Colorado at Boulder.

[§] University of California College of Medicine.

[||] Coordinates of the final structures have been deposited in the Protein Data Bank, Brookhaven National Laboratory, Upton, NY 11973, ID code 1BNB.

[⊗] Abstract published in *Advance ACS Abstracts,* October 1, 1995.

[1] Abbreviations: BNBD-12, bovine neutrophil β-defensin-12; NOE, nuclear Overhauser effect; RMSD, root mean square deviation; TAP, tracheal antimicrobial peptide; NMR, nuclear magnetic resonance spectroscopy; COSY, homonuclear correlation spectroscopy; DQF-COSY, double quantum filtered COSY; TOCSY, homonuclear total correlation spectroscopy; PECOSY, primitive exclusive COSY; NOESY, nuclear Overhauser effect spectroscopy; NP-2, rabbit neutrophil peptide two; NP-5, rabbit neutrophil peptide five; HNP-1, human neutrophil peptide one; HNP-2, human neutrophil peptide two; HNP-3, human neutrophil peptide three; GPNP, guinea pig neutrophil peptide; GAL-1, gallinacin one; GAL-2, gallinacin two.

0006-2960/95/0434-13663$09.00/0

structure, spacing of the conserved cysteines, and disulfide-bonding motif suggested that the β-defensins may have a novel tertiary structure.

The three-dimensional solution structure of BNBD-12 has been determined from ^{1}H-NMR data using distance geometry and restrained molecular dynamics to gain a better understanding of the β-defensins. This structure will be used to help understand the structural basis of the antimicrobial activity of the β-defensins. The structure of BNBD-12 will also be compared to the previously determined structures of the classical defensins and will be used to predict the structures of TAP and the gallinacin family of antimicrobial peptides.

MATERIALS AND METHODS

Sample Preparation. BNBD-12 was isolated from neutrophils obtained from an individual Hereford cow as described previously (Selsted et al., 1993). Five milligrams of purified peptide was dissolved in 550 μL of buffer to give a concentration of approximately 2.2 mM. The buffer consisted of 20 mM sodium succinate-d_4, 0.05 mM sodium ethylenediaminetetraacetic acid (EDTA), and 0.05 mM sodium azide in 90% H_2O/10% D_2O. After dissolution, the sample was adjusted to pH 4.0 at 25 °C. For experiments in D_2O, the above sample was first lyophilized to dryness, redissolved in 550 μL of 99.9% D_2O, and allowed to exchange for 1 h at 37 °C. The sample was then lyophilized to dryness and redissolved in 550 μL of 99.996% D_2O. The pH was checked and adjusted as necessary to 4.0 at 25 °C, without correcting for isotope effect.

NMR. All NMR experiments were performed on a Varian VXR-500S instrument operating at a proton frequency of 500 MHz. Spectra were obtained in phase-sensitive, absorption mode. The hypercomplex method was used for quadrature detection in the indirect dimension (States et al., 1982). The following homonuclear magnetic resonance experiments were collected using standard methods: COSY (Aue et al., 1976; Nagayama et al., 1980), DQF-COSY (Piantini et al., 1982; Rance et al., 1983), TOCSY (Bax & Davis, 1985; Braunschweiler & Ernst, 1983), PECOSY (Mueller, 1987), NOESY (Kumar et al., 1980; Macura & Ernst, 1980), and Triple Quantum (Rance & Wright, 1986). For experiments in H_2O, the H_2O signal was reduced by continuous preirradiation at low power for the final 1.2 s of the 1.5 s recycle delay used in all of the experiments. For TOCSY experiments, an 8.3 kHz spin-lock field was generated with the MLEV-16 composite pulse sequence (Bax & Davis, 1985). The spin-lock time was 35 or 77 ms as indicated and was preceded, and followed, by a 1 ms trim pulse. NOESY experiments were collected using mixing times of 50, 100, and 180 ms in both H_2O and D_2O. The spectral width was 6000 Hz in both dimensions for all experiments, except for the COSY experiment in H_2O which had a spectral width of 3500 Hz in the indirect dimension. COSY and PECOSY spectra were collected with 512 complex t_1 increments, 64 transients per increment, and 4096 complex points. TOCSY and NOESY experiments consisted of 220 complex t_1 increments, 64 transients per increment, and 2048 complex points.

All NMR data were transferred to a SiliconGraphics Iris 4D/35 computer for processing with the FELIX program (Biosym Technologies Inc.). Processing parameters for the NMR data included the following. For all H_2O spectra, the residual water signal was removed with low-frequency deconvolution (Marion et al., 1989). The COSY and PECOSY data were multiplied by a 30°-shifted sine bell window function in both dimensions and zero-filled in t_1 to give 2048 × 4096 real matrices. The first point in the t_1 dimension of the TOCSY and NOESY data was linear predicted to remove base line distortion. The t_1 dimension was then extended to 300 real points by linear prediction. Both dimensions were multiplied by a 60−80°-shifted skewed (0.4−0.6) sine bell window function. Finally, data were zero-filled in t_1 to give 1024 × 2048 real matrices.

Structural Constraints. The constraints used in the calculation of structures consisted of proton−proton distances derived from NOE cross-peaks, dihedral angles derived from proton−proton coupling constants using the Karplus relation, and hydrogen bond constraints for some slowly exchanging amide protons. Inter-proton distances were determined from the rate of buildup of the NOE cross-peaks. The 50 and 100 ms mixing time volume points were fit to a straight line to determine the rate of NOE buildup. While not experimentally measured, zero NOE volume at zero mixing time was also included as a data point in the fit. For NOEs from H_2O spectra, buildup rates were converted to distances by normalization to the average buildup rate of the three largest sequential HN−H_α NOE cross-peaks. This rate was scaled to 2.20 Å. For NOEs from D_2O spectra, distances were determined by normalizing the NOE buildup rate to the average buildup rate of the three largest resolvable H_β−H_β methylene NOEs. This rate was scaled to 1.80 Å. For the structure calculations, all inter-proton distances were given a lower bound of 1.80 Å. Inter-proton distances less than 2.50 Å were given an upper bound of 3.00 Å, distances greater than or equal to 2.50 Å and less than or equal to 3.00 Å had an upper bound of 4.50 Å, and distances greater than 3.00 Å were given an upper bound of 5.50 Å.

$^3J_{HN_\alpha}$ and $^3J_{\alpha\beta}$ coupling constants were measured in H_2O COSY and D_2O PECOSY, respectively. ϕ dihedral angle constraints were derived from the Karplus relation (Pardi et al., 1984). Residues with a $^3J_{HN_\alpha}$ coupling constant greater than 8.8 Hz were constrained to have backbone dihedral angle $\phi = -120 \pm 30°$. When $^3J_{\alpha\beta}$ couplings and NOE connectivities consistent with a particular side chain conformation were present, the appropriate χ_1 dihedral angle constraints of 60, −60, or $-180 \pm 20°$ were imposed (Basus, 1989).

Slowly exchanging amide protons indicate solvent inaccessibility and/or participation in hydrogen bonds (Englander & Kallenbach, 1983). Amide protons exhibiting slow deuterium for proton exchange kinetics were identified by lyophilization of a fully protonated sample in H_2O to dryness, redissolution in D_2O, and immediate collection of a 35 ms mixing time TOCSY experiment at 25 °C. Observation of HN−H_α cross-peaks for some residues indicated slow exchange of their amide protons. Some of the slowly exchanging amide protons were assigned hydrogen bond acceptors. Acceptors were assigned on the basis of NOE connectivities and initial structures calculated in the absence of H bond constraints. The majority of the acceptors were revealed by searching for oxygen atoms within a radius of 3.0 Å of the slowly exchanging amide protons in a family of structures calculated without H bond constraints. The remainder of the H bond acceptors were assigned later in

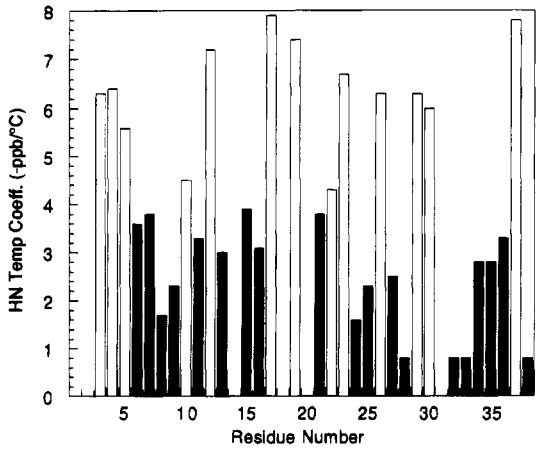

FIGURE 1: Measured temperature coefficients of the amide protons are plotted. The open bars denote random coil-like temperature coefficients. The filled bars indicate temperature coefficients less than −4 ppb/°C, which are consistent with those amide protons being protected from solvent (Jimenez et al., 1986). The intermediate temperature coefficients of G10 and R22 amide protons are discussed in the text.

the structure determination from more extensively constrained families of structures. Hydrogen bonds were constrained with two distance bounds, HN−O = 2.0 ± 0.4 Å and N−O = 3.0 ± 0.4 Å, and were treated as NOE constraints in terms of energy potentials and force constants.

Additional information about the chemical environment of the amide protons was obtained by measurement of amide temperature coefficients. Slowed exchange kinetics and low-temperature coefficients can indicate protection from solvent (Jimenez et al., 1986). The temperature coefficient is the slope of the line obtained by plotting the amide chemical shift versus temperature. Amide chemical shifts were measured in 35 ms mixing time TOCSY experiments acquired at 5, 15, 20, 25, 30, 35, and 45 °C. Chemical shifts were referenced to external TSP at 0 ppm over this temperature range. The chemical shift temperature coefficients of the amide protons of BNBD-12 are plotted in Figure 1.

Structure Calculations. All structure calculations were performed on a SiliconGraphics Indigo R4400 computer using the program XPLOR 3.1 (Brünger, 1992b). Three independent methods were used to search conformational space for a unique peptide fold. These methods were distance geometry (Brünger, 1992a), simulated annealing starting from an extended conformation (Nilges et al., 1991), and simulated annealing starting from randomized atom coordinates (Nilges et al., 1988). The structures from the above protocols were then regularized with simulated annealing (Nilges et al., 1992a) for 3000 steps of dynamics at 3000 K and then cooled to 300 K over 8000 steps with a 3 fs time step. The van der Waals term was purely repulsive and scaled upward during cooling. No electrostatics term was used in this protocol. The energy minimization employed the conjugate gradient method (Powell, 1977). The constraints used for the determination of the global fold of BNBD-12 consisted of the following: dihedral constraints for ϕ and χ derived from scalar J coupling constants and 26 tertiary distance constraints which were assigned unambiguously. No intraresidue, sequential, or hydrogen bond distance constraints were used in the determination of the global fold. The low-energy structures obtained by regularization of

Table 1: Distance Constraints for BNBD-12[a]

constraint type	no. of constraints	% of total
intraresidue	95	39
interresidue	147	61
<5 residues away	184	76
≥5 and <10 residues away	16	7
≥10 residues away	42	17
<2.50 Å	72	30
≥2.50 and <3.50 Å	132	54
≥3.50 Å	38	16

[a] Distance constraints are tabulated for all proton−proton and hydrogen bond distances used in the structure calculations of BNBD-12. The total number of constraints is 242, and the number of constraints per residue is 6.4.

starting structures generated by each of the three independent methods had the same +2X,−1 topology pattern for the β-sheet (Richardson, 1981) and the same overall fold. Because of the unambiguous nature of the constraints used and since distance geometry and simulated annealing from random atom coordinates are fundamentally different methods for searching conformation space, this topology was taken to be the correct global fold. Ambiguities in NOE assignments and hydrogen bond acceptors were then interpreted in the context of this structural fold and added to the constraint list to further restrain subsequent structures. The final list of distance constraints for BNBD-12 is broken down into categories and listed in Table 1.

After identification of the global fold, only distance geometry calculations followed by the above simulated annealing regularization protocol were used to generate new starting structures for further refinement. These starting structures were refined in three steps. The first step was simulated annealing (Nilges et al., 1992b) from 2000 to 200 K over 18 ps. The second refinement step was simulated annealing from 1000 to 100 K over 30 ps. These two protocols employed XPLOR's purely repulsive van der Waals potential (repel). The electrostatics potential was turned off. The output structures from the second refinement step were generally of low total energy and had no NOE violations >0.25Å. Structures that met these criteria were then subjected to a final refinement step of simulated annealing at a constant temperature of 300 K for 20 ps in 1 fs steps. This final protocol utilized a 6−12 Lennard-Jones potential. A dielectric constant of 3 was used for the electrostatic potential. The NOE force constant for all calculations was 50 kcal/mol·Å^2, and R^{-6} averaging of NOE constraints for degenerate methylene and methyl protons was employed. Additional information about parameters, potentials, and protocols can be found in the XPLOR 3.1 manual (Brünger, 1992b).

All output structures were viewed and analyzed on a SiliconGraphics Indigo2 computer using the InsightII software package (Biosym Technologies Inc.). The ribbon diagrams were produced with MOLSCRIPT (Kraulis, 1991).

RESULTS

Spin System Identification. The protons of BNBD-12 were assigned using methods developed by Wüthrich and coworkers (Wüthrich, 1986). Thirty-two spin systems containing an amide proton were identified in COSY and TOCSY spectra collected in H_2O. The side chain amide or amino protons of arginine (ϵNH), asparagine (γNH_2), lysine (ϵNH_3^+),

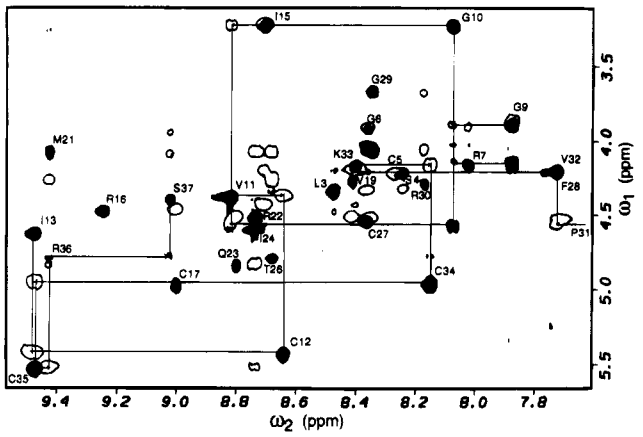

FIGURE 2: Contour plot of the HN−H_α region of the 180 ms mixing time NOESY spectrum in H_2O (open cross-peaks) is overlaid with the identical region of the 35 ms mixing time TOCSY spectrum in H_2O (filled cross-peaks). Two segments of $H_{\alpha[i]}$ to $HN_{[i+1]}$ connectivity are traced, G9 through I13 and P31 through S37. The H_α−HN cross-peaks are labeled with the residue assignments. The amide protons of N8, G25, and W38 resonate upfield of the plotted region.

and tryptophan (ϵNH) were also identified. Thirty-seven spin systems containing an H_α were identified in DQF-COSY and TOCSY spectra collected in D_2O. The aromatic protons of the phenylalanine and tryptophan residues were also identified. Where possible, degenerate methylene proton frequencies were confirmed in the Triple Quantum experiment spectrum.

Assignment of Resonances. The five proline residues in BNBD-12 divided the peptide chain into six sequential assignment segments. These segments were assigned using a 35 ms mixing time H_2O TOCSY spectrum overlaid with a 180 ms mixing time H_2O NOESY spectrum (Figure 2). Using the TOCSY spectrum, rather than the COSY, allowed rapid recognition of longer spin systems and facilitated the assignment process. The tandem glycine (G9 and G10) spin systems provided a unique marker for the P2 to I13 segment. Next, the short P14 to C17 segment was readily identified. The unique spin systems of M21 and Q23 marked the P20 to R30 segment. Finally, the extended K33 spin system followed by the dual AMX spin systems of C34 and C35 identified the C-terminal P31 to W38 segment. Following assignment of the individual segments, each segment was connected to its neighbors by $H_{\alpha[i]}$ to $H_{\delta/\delta'[\text{Proline } i+1]}$ NOE cross-peaks observed in a 180 ms mixing time NOESY spectrum collected in D_2O. A strong H_α−H_α NOE indicated a *cis*-peptide bond connecting V19 and P20. Finally, two NOE cross-peaks between the δ-protons of P2 and a previously unassigned resonance revealed the degenerate α-protons of G1 at 4.00 ppm. The sequential NOE connectivities in BNBD-12 are illustrated in Figure 3.

By combining $^3J_{\alpha\beta}$ coupling and NOE connectivity data, stereospecific assignment of some C_β methylene protons and valine C_γ methyl protons was possible using the method of Hyberts (Hyberts et al., 1987). For example, the C34H_β at 2.22 ppm had an H_α−H_β coupling of 12.2 Hz measured in the PE-COSY spectrum collected in D_2O. The other C34H_β at 2.38 ppm was measured to have a 3.6 Hz H_α−H_β coupling constant. The C34H_β at 2.22 ppm had a strong NOE cross-peak to the C34HN and a weak NOE cross-peak to the C34H_α in the 50 ms mixing time NOESY spectrum collected in H_2O. The C34H_β at 2.38 ppm displayed a weak NOE cross-peak to the C34HN and a strong NOE cross-peak to the C34H_α in the 50 ms NOESY spectrum. This combination of coupling constants and NOE cross-peaks is consistent with a t^2g^3 side chain conformation and a χ_1 dihedral angle of $-60 \pm 20°$ (Basus, 1989). Additionally, the C34H_β at 2.22 ppm was stereospecifically assigned as the pro-S β-proton, and the C34H_β at 2.38 ppm was assigned to the pro-R β-proton (Basus, 1989).

Tertiary Structure of BNBD-12. One hundred initial structures of BNBD-12 were calculated using distance geometry and simulated annealing. Fifty-one output structures with low total energy and no NOE violations greater than 0.25 Å were then further refined as described in Materials and Methods. Since all final structures had reasonable total energies, structures were evaluated on the basis of NOE constraint violation energy alone. The 20 structures with the lowest NOE violation energies were selected as the final ensemble of BNBD-12 structures. A backbone atom (N, C_α, and C) superimposition of the residues in the β-sheet (10−13, 22−27, and 32−36) for the final 20 structures is shown in Figure 4. As seen from the superimposition, some regions of the structure are more precisely defined than others. The N-terminal residues (1−4) are not displayed as they are poorly defined by the NMR data. The average pairwise RMSDs for residues 10−38 are as follows: backbone atoms = 0.93 ± 0.39 Å and all non-hydrogen atoms = 1.79 ± 0.49 Å. The backbone atoms of the residues in the β-strands (10−13, 22−27, and 33−36) are even more precisely defined with a pairwise RMSD of 0.45 ± 0.16 Å. The RMSDs for the backbone (N, C_α, and C) and for the non-hydrogen atoms of all residues are plotted in Figure 5. An average structure was calculated from the mean positions of the N, C_α, and C atoms of residues 10−38 in the final 20 structures. This structure was refined by simulated annealing from 1000 K to correct for problems with covalent geometry and is shown in Figure 6.

The global fold determined for BNBD-12 is a triple-stranded, antiparallel β-sheet of topology +2X,−1 (Richardson, 1981). This is very similar to the tertiary structures determined for all of the classical defensins investigated to date including NP-2, NP-5, HNP-1, and HNP-3 (Hill et al., 1991; Pardi et al., 1988, 1992). Residues G6−G9 form the first turn which is observed to be globally disordered relative to the rest of the structure. This turn is, however, rather well-defined locally with 19 of 20 structures having backbone

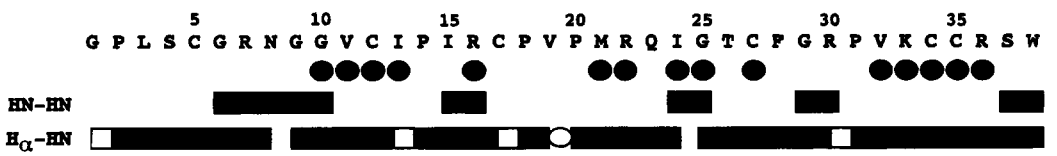

FIGURE 3: Sequential connectivities in BNBD-12 are diagrammed. $HN_{[i]}$ to $HN_{[i+1]}$ and $H_{\alpha[i]}$ to $HN_{[i+1]}$ interactions are denoted by filled bars. $H_{\alpha[i]}$ to $H_{\delta/\delta'[\text{proline } i+1]}$ connectivities are denoted by open squares. The open circle signifies a strong H_α−H_α NOE observed between V19 and P20. The filled circles indicate slowly exchanging amide protons.

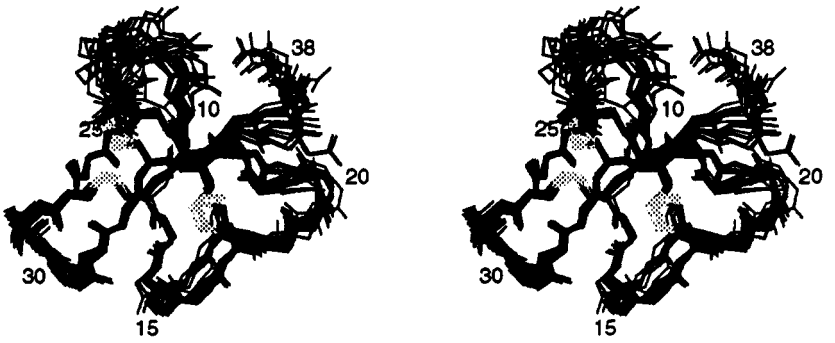

FIGURE 4: Stereoview of the superimposition of the 20 lowest NOE violation energy BNBD-12 structures is shown. The N, C_α, and C atoms were used to superimpose the residues of the β-sheet: G10−I13, R22−C27, and V32−R36. The N-terminal residues, G1−S4, are disordered and are not displayed. The N, C_α, C, and O atoms are displayed in black, and the three disulfide bonds are stippled.

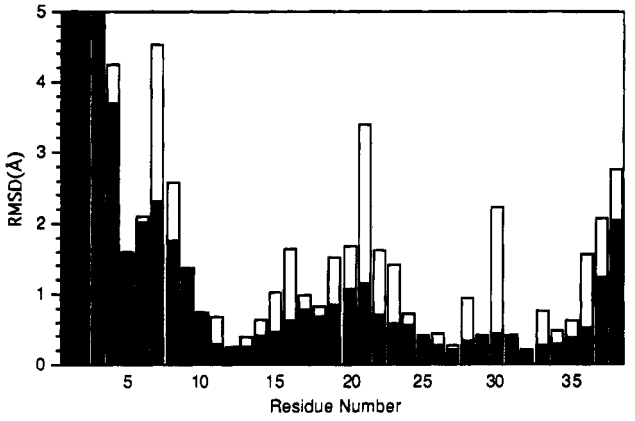

FIGURE 5: RMSD per residue for the backbone atoms, N, C_α, and C, are indicated by the filled bars. The open bars denote the RMSD per residue for all non-hydrogen atoms. RMSDs were calculated to the unminimized average structure calculated from the mean positions of the N, C_α, and C atoms of residues G10 through W38.

angles of $\phi_2 = -64 \pm 7°$ and $\psi_2 = -41 \pm 10°$ and $\phi_3 = -92 \pm 24°$ and $\psi_3 = -11 \pm 24°$ which define it as an ideal type I β-turn (Chou & Fasman, 1977). The other structure had some backbone angles for this turn that lie in a different conformational well. G6O and G9N are within hydrogen-bonding distance (average = 3.40 ± 0.35 Å). Although G9HN was not observed to be slowly exchanging, its temperature coefficient is reduced at −2.3 ppb/°C, suggesting weak protection from solvent. The N-terminal β-strand contains residues G10 through I13. Residues I13−R16 form a nonideal type II β-turn with 18 of 20 structures having backbone angles of $\phi_2 = -78 \pm 1°$ and $\psi_2 = 173 \pm 4°$ and $\phi_3 = 58 \pm 4°$ and $\psi_3 = -108 \pm 15°$. The average I13O−R16N distance is 5.14 ± 0.31 Å, too long for a hydrogen bond. The average P14O−R16N distance, however, is 3.08 ± 0.70 Å. R16HN was observed to have slightly faster exchange kinetics than the other slowly exchanging amide protons and was not constrained with a hydrogen bond to I13O or P14O. C17 separates the second and third turn. Residues P18−M21 form turn three which is a type VI turn containing a *cis*-proline at position 3 (Richardson, 1981). The mean backbone angles for this turn in all structures are $\phi_2 = -67 \pm 17°$ and $\psi_2 = 152 \pm 5°$ and $\phi_3 = -45 \pm 12°$ and $\psi_3 = -91 \pm 13°$. These angles are similar to other type VI β-turns with a *cis*-proline at position i+2 (Chou & Fasman, 1977). M21HN is slowly exchanging and was constrained to be within hydrogen-bonding distance of P18O. The average P18O−M21N distance observed was 2.78 ± 0.10 Å. Residues R22 and Q23 begin the second β-strand. The backbone of this strand makes a turn of approximately 80° at a β-bulge involving residues I24, G25, and C34. These backbone angles fall in ϕ, ψ space indicative of the classic type β-bulge described by Richardson (Richardson et al., 1978). Moreover, these angles lie within a subset of the classic type β-bulge of which the majority have a glycine at position 2 (Richardson et al., 1978). Residues T26 and C27 complete the second β-strand. Residues V32 through R36 were observed to have large $^3J_{HN-H_\alpha}$ coupling constants ($^3J_{HN-H_\alpha} \geq 9.3$ Hz) and were, therefore, constrained to have β-strand backbone geometry ($\phi = -120 \pm 30°$). These residues form the C-terminal β-strand in the triple-stranded sheet. The second and C-terminal strands form a β-hairpin secondary structure motif. The residues F28−P31 form a loop linking the two strands. Similar four-residue loops have been previously observed in crystal structures, including that of penicillopepsin (Sibanda & Thornton, 1985). The structure of a β-hairpin with this type of loop has been described as the hood of an erect cobra, because of the unique bend of the loop (Sibanda & Thornton, 1985), and is clearly visible

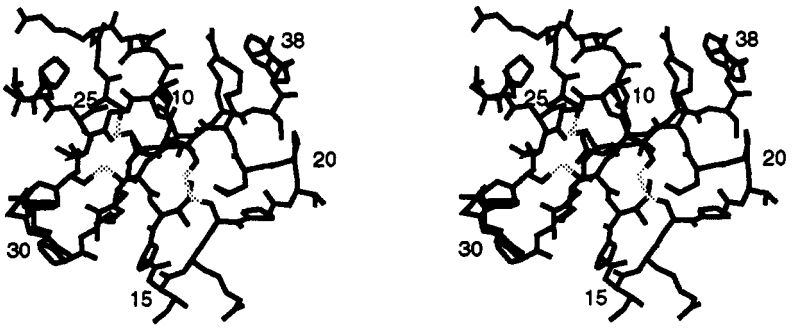

FIGURE 6: Stereoview of the minimized average structure of BNBD-12 is shown with all heavy atoms displayed. The three disulfide bonds are shown with stippled lines.

in the structure of BNBD-12. There were no tertiary NOEs to which we could attribute this conformation of turn four. Also, the same conformation was observed in preliminary structures calculated without electrostatic or Van der Waals potentials. The presence of a proline at position 4 of the turn may be affecting the backbone conformation of this turn.

The disulfide linkages (5−34, 12−27, and 17−35) previously determined biochemically (Tang & Selsted, 1993) were confirmed by NOE interactions. These interactions include an NOE between the H_α of C5 and the $H_\beta R$ of C34 and an NOE between the $H_\beta R$ of C12 and the $H_\beta R$ of C27. The three disulfides had $C_\alpha-C_\alpha$ and $C_\beta-C_\beta$ distances and dihedral angles similar to those observed in 72 disulfides from crystal structures (Srinivasan et al., 1990).

DISCUSSION

Structure of BNBD-12. The superimposition of the 20 lowest NOE violation energy structures shown in Figure 4 reveals a precisely defined triple-stranded, antiparallel β-sheet as the structural core of BNBD-12. The constraint list generated from the NMR spectra of BNBD-12 was consistently able to produce structures with low constraint violation energy and good van der Waals packing of side chains. Relative to the β-sheet, the global positions of the turns in BNBD-12 are not as well-defined. Superimpositions of the turns themselves, however, reveal that they are locally well-defined units, with geometries corresponding to turn types previously described for β-turns in crystal structures (Chou & Fasman, 1977). The RMSDs on a per residue basis for these structures, relative to an average structure calculated from the mean positions of the N, Cα, and C atoms of residues 10−38, are plotted in Figure 5.

The N-terminal strand of BNBD-12 was found to be disordered due to an absence of assignable long range NOEs for this region. The lack of assignable NOEs may be a result of the dynamic nature of this part of the molecule in solution. However, there is some evidence that the N-terminal residues may form a fourth antiparallel β-strand. First, there were some NOEs to residues in the N-terminal strand which could not be unambiguously assigned. Specifically, we were unable to corroborate a tentative L3HN−V32H_α NOE with additional interstrand NOEs. This constraint was left out of structure calculations but suggests a possible positioning of the N-terminal strand. The amide proton of C12, on the solution side of the N-terminal β-strand, exhibited slowed exchange kinetics. This observation is suggestive of hydrogen bonding, perhaps to the N-terminal strand. The temperature coefficient measured for C12HN (−7.2 ppb/°C), however, was not consistent with hydrogen bonding. A fourth β-strand could position the hydrophobic side chains of P2 or L3 to interact with the side chains of I13 and I15 in turn two. The other members of the β-defensin family also have amino acids at these positions which could form similar hydrophobic interactions. Finally, the majority of the β-defensin family, BNBD-3 through BNBD-7, BNBD-9, and BNBD-10, have an additional five-residue conserved N-terminal domain not present in BNBD-12. We expect that, in the case of these larger β-defensins, the region of sequence corresponding to the N-terminal strand of BNBD-12 will be more ordered. Together, the above observations suggest that the actual global topology of the β-defensin consensus may be +1,+2X,−1.

The exchange kinetics of the amide protons contain information about the local structure and dynamics of a peptide. Fifteen amide protons in the structure of BNBD-12 were observed to have slowed exchange kinetics (see Materials and Methods). This was taken to indicate secondary or tertiary interactions involving these amide protons (Englander & Kallenbach, 1983). The slowly exchanging amide protons of BNBD-12 are indicated in Figure 3. The temperature dependence of amide proton chemical shifts was used to confirm the hydrogen exchange results. Twelve of the fifteen slowly exchanging amide protons indicated in Figure 3 had temperature coefficients less than −4 ppb/°C. This indicates that these amide protons are protected from interaction with solvent (Jimenez et al., 1986). The slowly exchanging amide proton of C12 was discussed above. The slowly exchanging amide protons of G10HN and R22HN had temperature coefficients of −4.5 and −4.3 ppb/°C, respectively. These amide protons lie at an end of two separate β-strands and were constrained with hydrogen bonds. Their intermediate temperature coefficients, however, suggest that these hydrogen-bonding interactions at the ends of these β-strands may be transient in nature. It is interesting to note that the temperature coefficients of F28HN and W38HN are less than −1 ppb/°C; however, in the ensemble of BNBD-12 structures presented here, these amides appear to be fully accessible to solvent. Thus, the structure described here is not consistent with the standard interpretation of the amide temperature coefficient for these residues.

Most of the charged residues of BNBD-12, including R22, R30, K33, and R36, are on the β-hairpin face of the peptide. Possible exceptions are R7 and R16 which are present in turns one and two, respectively; however, these arginine side chains are disordered in the ensemble of BNBD-12 structures. The opposite face, composed of the N-terminal region of the peptide, is nearly completely hydrophobic in nature. This cationic/hydrophobic polarity was noted in the case of HNP-3 by Hill and Eisenberg (Hill et al., 1991) and in the case of HNP-1 by Pardi et al. (1992). The cationic nature of the defensins is one of their defining characteristics (Lehrer et al., 1993). Coupled with the fact that defensins require oxidized disulfides and therefore, presumably, an intact structure to elicit antimicrobial activity (Lehrer et al., 1985), the above observations reinforce the hypothesis that the cationic/hydrophobic amphiphilicity of the defensins is the structural basis of the mechanism by which they interact with their target.

Similarity of Classical and β-Defensins. On the basis of nucleotide sequence and primary structure, the β-defensins were initially modeled to have a tertiary structure similar to that of the classical defensins (M. E. Selsted, unpublished results). The different disulfide linkage motif determined for the BNBD-12, however, presented the possibility that the β-defensins could have a unique tertiary structure relative to the classical defensins (Tang & Selsted, 1993). As illustrated in a comparison of ribbon diagrams (Figure 7), the similarity between BNBD-12 and NP-2, a representative of the classical defensin family, is striking. With the exception of the additional N-terminal strand in the β-defensin, the structures are nearly superimposable. A superimposition of the backbone atoms of the residues in the β-strands (RMSD = 1.78 Å, results not shown) reveals that, while the classical and β-defensins have different disulfide linkages, 1−5, 2−4, and 3−6 in the β-defensins and 1−6,

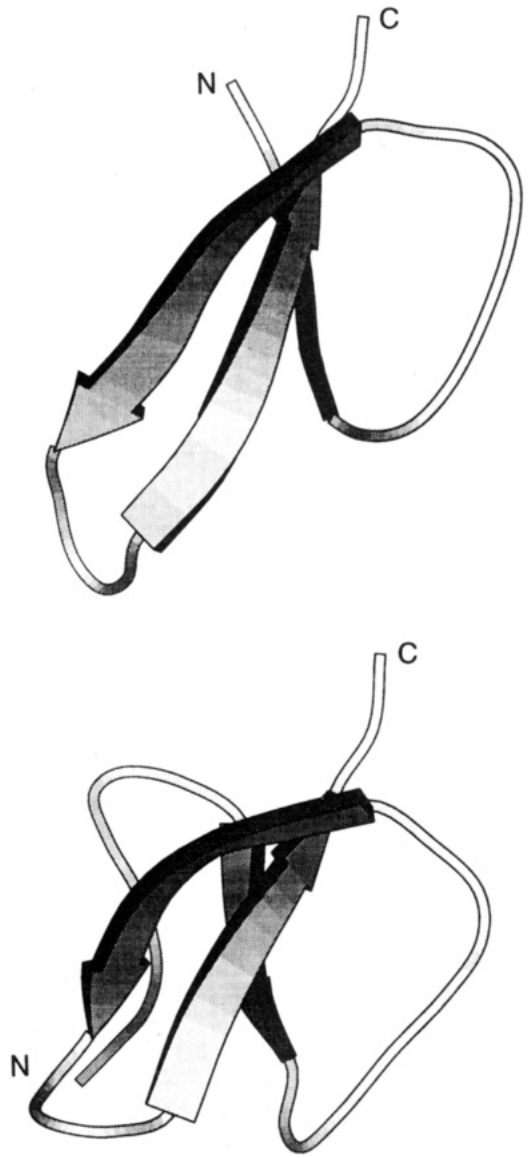

FIGURE 7: Three-dimensional solution structures of BNBD-12, a β-defensin (bottom), and NP-2 (Pardi et al., 1992), a classical defensin (top), are presented as MOLSCRIPT ribbon diagrams (Kraulis, 1991).

2−4, and 3−5 in the classical defensins, the disulfides occur at nearly identical spatial locations in the tertiary structures.

Residues R6 and E14 are conserved in all of the classical defensins, except GPNP from guinea pig (Selsted & Harwig, 1987). These residues were observed to form a salt bridge in the crystal structure of HNP-3 (Hill et al., 1991). There are no such complementary charged residues in analogous positions (17 and 25) in the β-defensin consensus. In this region, however, BNBD-12 has a well-ordered (side chain RMSD < 1.0 Å) network of hydrophobic interactions. The residues involved include I13, C17, P18, and C35. This hydrophobic network in the β-defensins replaces the electrostatic salt bridge of the classical defensins and is likely helping to stabilize the tertiary structure of the β-defensins.

In an ensemble of NP-2 (a classical defensin) solution structures, the first turn (analogous to turn two in the β-defensins) is locally well-defined but globally disordered (Pardi et al., 1992). This arises from an absence of NOEs tying this turn to the remainder of the structure. This lack of NOEs may be due to the flexibility of this region of the peptide in solution (Pardi et al., 1992). In comparison, turn two of BNBD-12 is both locally (type II) and globally well-defined. The global placement of this turn was determined by strong NOEs between the H_α of V32 and the H_α and HN of P14 and I15, respectively.

A G-X-C motif in the middle of the second strand of the β-sheet is conserved in both the classical and β-defensins (Figure 8). In both families, it is observed to form a β-bulge structure. In the crystal structure of HNP-3, this β-bulge is necessary for positioning the backbone for a water-mediated hydrogen bond across the dimer interface (Hill et al., 1991). The presence of a β-bulge in BNBD-12 suggests that, like the classical defensins, the β-defensins may also form a dimer structure. A β-bulge preceding a β-hairpin is often used by protein structures to establish an interaction site on one side of a β-sheet; examples can be found in the immunoglobulins and prealbumin (Richardson, 1981). The defensins may use this structural motif to mediate multimer interactions and/or to bind their target. No intermolecular NOEs, however, were observed in any of the NOESY spectra of BNBD-12. More importantly, neither of the amide protons on the putative HNP3-type dimer interface (T26 and F28 in BNBD-12) was found to be slowly exchanging. The presence of slowly exchanging amide protons at positions predicted to be protected from solvent by the X-ray structure of the HNP-3 dimer was consistent with the classical defensins NP-2 and HNP-1 forming dimers in solution (Pardi et al., 1992). F28HN of BNBD-12 did have a temperature coefficient less than −1 ppb/°C, which is indicative of protection. Overall, there is no convincing NMR evidence to support a BNBD-12 dimer structure. The possibility remains, however, that a dimer could be the active form of BNBD-12. It is generally thought that the defensins interact with the cell membrane. Perhaps there is a much greater tendency for defensins to aggregate into dimers or higher order multimers in a membrane environment than in aqueous solution. Biochemical studies of the interactions of human defensins (classical type) with lipid membranes suggest that the classical defensins can form multimeric porelike structures. Kagan et al. (1990) showed that HNP-1 and -2 can form voltage-dependent channels in a planar lipid bilayer. More recently, Wimley et al. (1994) have presented evidence that HNP-2 can form multimeric pores in unilamellar lipid vesicles.

The conserved β-bulge in the defensins may simply be necessary for establishing the proper register of side chains for folding or for antimicrobial activity. The hydrophilic residue T26 (this is the conserved residue T30 in the β-defensin consensus) immediately follows the β-bulge in the structure of BNBD-12. In the absence of the β-bulge, this side chain would point toward the hydrophobic interior of the peptide. This residue is observed to have a well-ordered side chain in an ensemble of BNBD-12 structures, with the O_γ pointing into the putative HNP3-type dimer interface. This oxygen could accept a hydrogen bond from a side chain or the backbone of the other monomer in a dimer structure. Alternatively, this threonine side chain could have an important functional role. It is interesting to note that BNBD-1, which has an isoleucine mutation at this position, has severely reduced activity relative to the other members of the β-defensin family (Selsted et al., 1993). Site-specific mutagenesis experiments of this residue in a BNBD-12 background are currently in progress to elucidate the functional significance of this side chain.

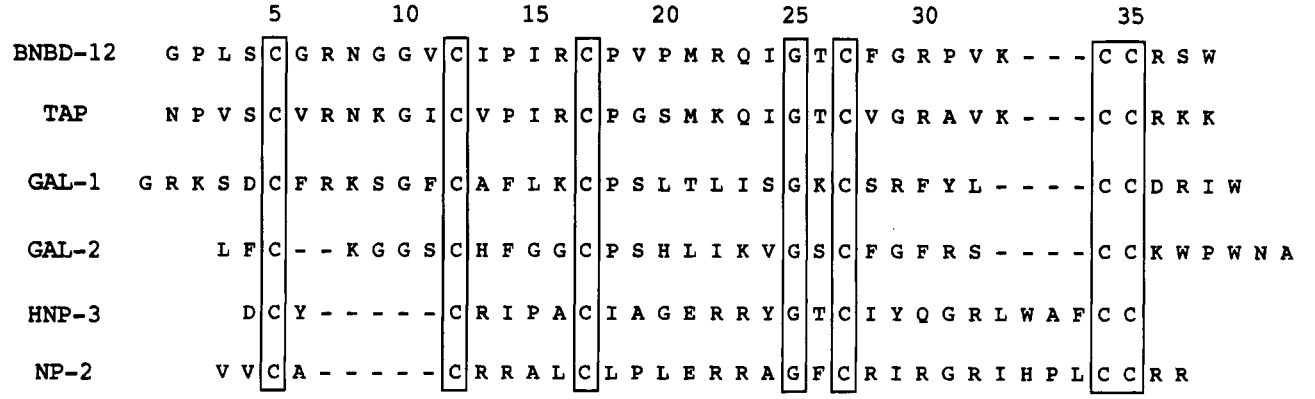

FIGURE 8: Maximized alignment of the primary structures of BNBD-12, TAP, two gallinacins (GAL-1 and GAL-2), and two classical defensins (HNP-3 and NP-2) is shown. The alignment was maximized for the six cysteine residues by addition of gaps in the C-terminal region of the β-defensins and in the N-terminal region of the classical defensins. Note also the conserved glycine residue which is observed to be involved in a β-bulge in the structures of BNBD-12, HNP-3, and NP-2.

Peptides nearly identical to BNBD-12 have recently been isolated from bovine trachea and the leukocytes of chickens. TAP isolated from bovine trachea shares 66% sequence identity with BNBD-12 (Diamond et al., 1991). Gallinacins, a family of antimicrobial peptides isolated from chicken leukocytes, share a core of nine invariant residues with the β-defensins (Harwig et al., 1994). A primary structure comparison of BNBD-12, TAP, two gallinacins, and two classical defensins is shown in Figure 8. We predict that TAP and the gallinacins will have tertiary structures very similar to that described here for BNBD-12.

Although the classical and β-defensins have different primary structures and nucleotide sequences, the similarity of their tertiary structures is good evidence that they have diverged from a common defense peptide, because tertiary structure diverges more slowly than primary structure (Matthews et al., 1981). The recent identification of the gallinacins from chicken leukocytes is striking. These cysteine-rich antimicrobial peptides share a nine-residue "core motif" with the β-defensins, including the six cysteines, two glycines, and a proline (Harwig et al., 1994). This proline is P18 in the BNBD-12 sequence, which is observed to participate in an important hydrophobic interaction network as discussed above. The conservation of this residue across the β-defensins and the gallinacins suggests that the two families may be using similar interactions to stabilize their structures. The above considerations suggest that the core structural motif of the β-defensins and its inherent antimicrobial activity may have evolved prior to the divergence of the mammalian and avian lines 250 million years ago (Harwig et al., 1994). The similarity of the defensins to the sapecins (insect defensins) (Hanzawa et al., 1990) and scorpion charybdotoxins (Bontems et al., 1991) is more striking still. The peptides of these families are nearly identical in size, with each having three disulfides, including a shared 3−6 linkage. They also share the conserved glycine in a β-bulge initiating a β-hairpin secondary motif. The speculation that all of these families have diverged from a common defense peptide developed prior to the divergence of mammals and insects is tempting. Proof of this speculation would underscore the importance of peptide-mediated immunity in the development of higher organisms (Boman, 1991). The ability to destroy infecting bacteria or fungi was certainly a useful adaptation during the development of muticellular organisms. The structure of the defensins may be a look at one of the first weapons of the innate immune system, a weapon so simple and effective that it remains today. Another possibility, however, remains. These families of defense peptides may simply have converged on a small, highly stable tertiary structure for the presentation of active side chain functional groups.

ACKNOWLEDGMENT

We thank Drs. E. P. Nikonowicz and J. J. Skalicky for helpful discussions.

NOTE ADDED IN PROOF

Bensch et al. have recently reported the isolation of a human β-defensin from the plasma ultrafiltrate of individuals undergoing renal dialysis. This is the first example of the coexistence of classical defensin and β-defensin genes in any species [Bensch, K. W., Raida, M., Mägert, H.-J., Schulz-Knappe, P., & Forssmann, W. G. (1995) *FEBS Lett. 368*, 331−335].

SUPPORTING INFORMATION AVAILABLE

Four tables containing proton resonance assignments, coupling constants and dihedral constraints, hydrogen bond distance constraints, and proton−proton distance constraints (10 pages). Ordering information is given on any current masthead page.

REFERENCES

Aue, W. P., Bartholdi, E., & Ernst, R. R. (1976) *J. Chem. Phys. 64*, 2229−2246.
Bach, A. C., II, Selsted, M. E., & Pardi, A. (1987) *Biochemistry 26*, 4389−4397.
Basus, V. J. (1989) *Methods Enzymol. 177*, 132−149.
Bax, A., & Davis, D. G. (1985) *J. Magn. Reson. 65*, 355−360.
Boman, H. G. (1991) *Cell 65*, 205−207.
Bontems, F., Roumestand, C., Gilquin, B., Menez, A., & Toma, F. (1991) *Science 254*, 1521−1523.
Braunschweiler, L., & Ernst, R. R. (1983) *J. Magn. Reson. 53*, 521−528.
Brünger, A. T. (1992b) *X-PLOR 3.1: A System for X-ray Crystallography and NMR*, Yale University Press, New Haven and London.
Chou, P. Y., & Fasman, G. D. (1977) *J. Mol. Biol. 115*, 135−175.
Diamond, G., Zasloff, M., Eck, H., Brasseur, M., Maloy, W. L., & Bevins, C. L. (1991) *Proc. Natl. Acad. Sci. U.S.A. 88*, 3952−3956.

Eisenhauer, P. B., Harwig, S. S., Szklarek, D., Ganz, T., Selsted, M. E., & Lehrer, R. I. (1989) *Infect. Immun. 57*, 2021−2027.
Englander, S. W., & Kallenbach, N. R. (1983) *Q. Rev. Biophys. 16*, 521−655.
Ganz, T., Selsted, M. E., Szklarek, D., Harwig, S. S., Daher, K., Bainton, D. F., & Lehrer, R. I. (1985) *J. Clin. Invest. 76*, 1427−1435.
Hanzawa, H., Shimada, I., Kuzuhara, T., Komano, H., Kohda, D., Inagaki, F., Natori, S., & Arata, Y. (1990) *FEBS Lett. 269*, 413−420.
Harwig, S. S., Swiderek, K. M., Kokryakov, V. N., Tan, L., Lee, T. D., Panyutich, E. A., Aleshina, G. M., Shamova, O. V., & Lehrer, R. I. (1994) *FEBS Lett. 342*, 281−285.
Hill, C. P., Yee, J., Selsted, M. E., & Eisenberg, D. (1991) *Science 251*, 1481−1485.
Hyberts, S. G., Marki, W., & Wagner, G. (1987) *Eur. J. Biochem. 164*, 625−635.
Jimenez, M. A., Nieto, J. L., Rico, M., Santoro, J., Herranz, J., & Bermejo, F. J. (1986) *J. Mol. Struct. 143*, 435−438.
Kagan, B. L., Selsted, M. E., Ganz, T., & Lehrer, R. I. (1990) *Proc. Natl. Acad. Sci. U.S.A. 87*, 210−214.
Kraulis, P. J. (1991) *J. Appl. Crystallogr. 24*, 946−950.
Kumar, A., Ernst, R. R., & Wüthrich, K. (1980) *Biochem. Biophys. Res. Commun. 95*, 1−6.
Lehrer, R. I., Daher, K., Ganz, T., & Selsted, M. E. (1985) *J. Virol. 54*, 467−472.
Lehrer, R. I., Lichtenstein, A. K., & Ganz, T. (1993) *Annu. Rev. Immunol. 11*, 105−128.
Macura, S., & Ernst, R. R. (1980) *Mol. Phys. 41*, 95−117.
Marion, D., Ikura, M., & Bax, A. (1989) *J. Magn. Reson. 84*, 425−430.
Matthews, B. W., Remington, S. J., Grütter, M. G., & Anderson, W. F. (1981) *J. Mol. Biol. 147*, 545−558.
Mueller, L. (1987) *J. Magn. Reson. 72*, 191−196.
Nagayama, K., Kumar, A., Wüthrich, K., & Ernst, R. R. (1980) *J. Magn. Reson. 40*, 321−334.
Nilges, M., Clore, G. M., & Gronenborn, A. M. (1988) *FEBS Lett. 239*, 129−136.
Nilges, M., Kuszewski, J., & Brünger, A. T. (1991) *Computational Aspects of the Study of Biological Macromolecules by NMR*, Plenum Press, New York.
Ouellette, A. J., Miller, S. I., Henschen, A. H., & Selsted, M. E. (1992) *FEBS Lett. 304*, 146−148.
Pardi, A., Billeter, M., & Wüthrich, K. (1984) *J. Mol. Biol. 180*, 741−751.
Pardi, A., Hare, D. R., Selsted, M. E., Morrison, R. D., Bassolino, D. A., & Bach, A. 2. (1988) *J. Mol. Biol. 201*, 625−636.
Pardi, A., Zhang, X. L., Selsted, M. E., Skalicky, J. J., & Yip, P. F. (1992) *Biochemistry 31*, 11357−11364.
Piantini, U., Sørensen, O. W., & Ernst, R. R. (1982) *J. Am. Chem. Soc. 104*, 6800−6801.
Powell, M. J. D. (1977) *Mathematical Programming 12*, 241−254.
Rance, M., & Wright, P. E. (1986) *J. Magn. Reson. 66*, 372−378.
Rance, M., Sørensen, O. W., Bodenhausen, G., Wagner, G., Ernst, R. R., & Wüthrich, K. (1983) *Biochem. Biophys. Res. Commun. 117*, 479−485.
Richardson, J. S. (1981) *Adv. Protein Chem. 34*, 167−339.
Richardson, J. S., Getzoff, E. D., & Richardson, D. C. (1978) *Proc. Natl. Acad. Sci. U.S.A. 75*, 2574−2578.
Selsted, M. E., & Harwig, S. S. (1987) *Infect. Immun. 55*, 2281−2286.
Selsted, M. E., & Harwig, S. S. (1989) *J. Biol. Chem. 264*, 4003−4007.
Selsted, M. E., Brown, D. M., DeLange, R. J., Harwig, S. S., & Lehrer, R. I. (1985) *J. Biol. Chem. 260*, 4579−4584.
Selsted, M. E., Tang, Y. Q., Morris, W. L., McGuire, P. A., Novotny, M. J., Smith, W., Henschen, A. H., & Cullor, J. S. (1993) *J. Biol. Chem. 268*, 6641−6648.
Sibanda, B. L., & Thornton, J. M. (1985) *Nature 316*, 170−174.
Srinivasan, N., Sowdhamini, R., Ramakrishnan, C., & Balaram, P. (1990) *Int. J. Pept. Protein Res. 36*, 147−155.
States, D. J., Haberkorn, R. A., & Ruben, D. J. (1982) *J. Magn. Reson. 48*, 286−292.
Tang, Y.-Q., & Selsted, M. E. (1993) *J. Biol. Chem. 268*, 6649−6653.
Territo, M. C., Ganz, T., Selsted, M. E., & Lehrer, R. I. (1989) *J. Clin. Invest. 84*, 2017−2020.
Tominaga, T., Fukata, J., Naito, Y., Nakai, Y., Funakoshi, S., Fujii, N., & Imura, H. (1990) *J. Endocrin. 125*, 287−292.
Wimley, W. C., Selsted, M. E., & White, S. H. (1994) *Protein Sci. 9*, 1362−1373.
Wüthrich, K. (1986) *NMR of Proteins and Nucleic Acids*, John Wiley & Sons, New York.
Zhang, X. L., Selsted, M. E., & Pardi, A. (1992) *Biochemistry 31*, 11348−11356.

BI951035S